Original article
EDN: RWHVLN
DOI: 10.21285/2686-9993-2026-49-2-4

Monitoring interannual variations in ice conditions of Lake Kulinda in April based on Landsat-8 and Landsat-9 time-series imagery

Mengyao Gu[a]✉, Xiangyu Meng[b], Vladimir M. Zhulikov[c], Vitaliy L. Ruposov[d]

[a,b]Henan Polytechnic University, Jiaozuo, China
[c,d]Irkutsk National Research Technical University, Irkutsk, Russian Federation

Abstract. The ice conditions of lakes serve as an indicator of regional climate change. This study focuses on Lake Kulinda, located at the northern end of Lake Baikal, Russia. The study analyzes the patterns of ice melting in this lake in April 2019, 2021, 2023, and 2025, and identifies the factors influencing the evolution of ice lakes in this region using Landsat-8 and Landsat-9 remote sensing data and GIS analysis tools. The results show that between 2019 and 2025, the ice cover of Lake Kulinda decreased from 9.17 km² to 8.86 km², resulting in a total reduction of 0.31 km² with an average annual decrease of 0.05 km². The rate of ice melting initially increased and then decreased. The largest annual reduction was observed in the period 2021–2023 (0.08 km²), while in the period 2023–2025 the rate slowed down (0.04 km²), which indicates a slowdown in the dynamics of the lake's ice cover. The retreat of the ice cover occurred along the coastal zones, especially in the southeastern and northwestern parts, while the central part remained covered with ice. The boundary between ice and open water gradually shifted towards the center of the lake every year. Changes in the area of the ice cover are associated with the warming climate of the region. The phases of rapid melting in 2021–2023 coincided with the statistical spring warming, and the subsequent slowdown is related to the nonlinear interaction between natural climate fluctuations and the dynamics of the ice cover. This indicates the adaptive capabilities and self-regulation of the lake's ice cover. The research results can be used in monitoring the phenological state of the ice cover formation in the lakes of the Northern Baikal region, which will contribute to a better understanding of climate change in the region.

Keywords: Lake Kulinda, lake ice phenology, Landsat-8, Landsat-9, normalized difference snow index, interannual variation

For citation: Gu M., Meng X., Zhulikov V.M., Ruposov V.L. Monitoring interannual variations in ice conditions of Lake Kulinda in April based on Landsat-8 and Landsat-9 time-series imagery. *Earth sciences and subsoil use.* 2026;49(2):?-?. https://doi.org/10.21285/2686-9993-2026-49-2-4.

Научная статья
УДК 556

Анализ многолетних изменений ледовой обстановки на озере Кулинда в апреле с использованием данных с космических спутников Landsat-8 и Landsat-9

М. Гу[a]✉, С. Мэн[b], В.М. Жуликов[c], В.Л. Рупосов[d]

[a,b]Хэнаньский политехнический университет, Цзяоцзо, Китай
[c,d]Иркутский национальный исследовательский технический университет, Иркутск, Российская Федерация

Резюме. Ледовая обстановка озер служит индикатором региональных климатических изменений. В данном исследовании рассматривается оз. Кулинда, расположенное в северной оконечности оз. Байкал в России. В исследовании проанализированы закономерности таяния льда на этом озере в апреле 2019, 2021, 2023 и 2025 гг. и выявлены факторы, влияющие на эволюцию ледяных озер в рассматриваемом регионе с использованием данных дистанционного зондирования спутниками Landsat-8 и Landsat-9 и инструментов геоинформационной системы анализа. Полученные результаты показывают, что в период с 2019 по 2025 г. площадь ледяного покрова оз. Кулинда уменьшилась с 9,17 до 8,86 км², что составляет суммарное сокращение на 0,31 км² при среднем годовом уменьшении 0,05 км². Скорость таяния льда сначала увеличивалась, а затем снизилась. Наибольшее годовое сокращение ледового покрова наблюдалось в период с 2021 по 2023 г. (0,08 км²), тогда как в период с 2023 по 2025 г. скорость снизилась (0,04 км²), что указывает на замедление динамики ледового покрова озера. Отступление ледяного покрова происходило вдоль прибрежных зон, особенно в юго-восточных и северо-западных частях, тогда как центральная часть оставалась покрытой льдом. Граница между ледовым покровом и открытой водой каждый год постепенно смещалась к центру озера. Изменения площади ледяного покрова связаны с потеплением климата в регионе. Фазы быстрого таяния льда в период с 2021 по 2023 г. совпали со статистическим весенним потеплением, а последующее замедление связано с нелинейным взаимодействием между естественными климатическими колебаниями и динамикой ледового покрова. Это свидетельствует об адаптационных возможностях и саморегуляции ледяного покрова озера. Результаты исследований могут быть использованы для мониторинга фенологического состояния образования и разрушения ледового покрова озер Северного Прибайкалья, что будет способствовать лучшему пониманию изменений климата в регионе.

Ключевые слова: озеро Кулинда, фенология ледяного покрова, Landsat-8, Landsat-9, нормализованный разностный индекс снежного покрова, межгодовые вариации

Для цитирования: Гу М., Мэн С., Жуликов В.М., Рупосов В.Л. Анализ многолетних изменений ледовой обстановки на озере Кулинда в апреле с использованием данных с космических спутников Landsat-8 и Landsat-9 // Науки о Земле и недропользование. 2026. Т. 49. № 2. С. ?–?. https://doi.org/10.21285/2686-9993-2026-49-2-4.

Introduction

Global climate change is currently attracting widespread attention. However, the degree of human influence on this process and on its overall trend remains difficult to determine. Therefore, studying climate change in densely populated urban areas helps assess the impact of human activities on the global climate. At the same time, observations and records from sparsely populated regions are important for further evaluation of human influence. Since ground observations in remote areas are difficult, remote sensing can be used to monitor key indicators of climate change from a distance. The aim of this study is to analyze long-term changes in the ice cover of Lake Kulinda in order to identify climate-change trends. The study area is Lake Kulinda in the Republic of Buryatia, Russia. The nearest settlement is the village of Kichera, located 30 km north of Lake Baikal, which makes the study area sparsely populated (Fig. 1).

The typical continental Baikal region is characterized by synchronous changes in ice phenology, which manifests itself in the fact that mountain lakes tend to experience shorter periods of ice formation and smaller ice cover areas at earlier times [1–3]. The ice regime of Lake Kulinda clearly confirms the trend of spring degradation of lake ice in the Baikal region. Consequently, the results of this study can be used

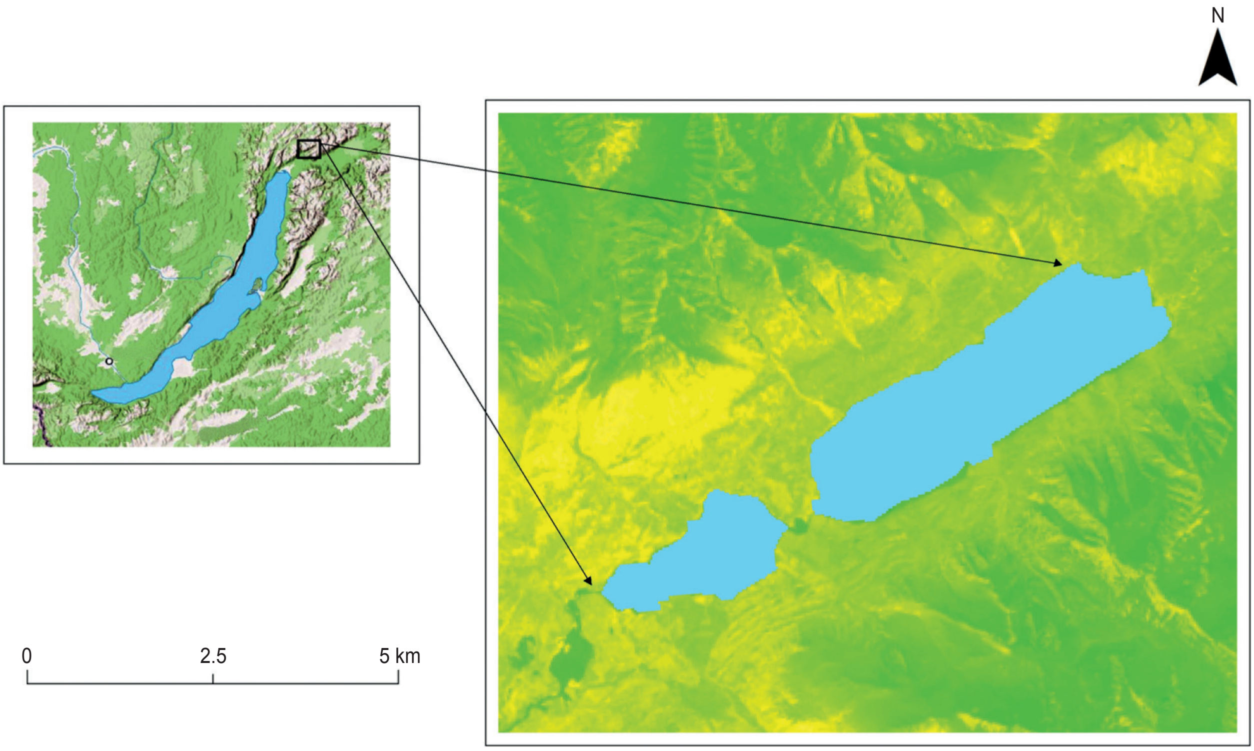

a *b*

Fig. 1. Study area:
a – 56°06’ N; b – 110°29’ E
Рис. 1. Район исследования:
a – 56°06’ с. ш.; b – 110°29’ в. д.

to obtain new scientific data for studying the evolution of climatic-hydrological processes in the region [4–7]. Considering the geographical location and conditions of Lake Kulinda (Fig. 2), satellite data–with their advantages of average spatial resolution, multispectral capability, and convenient visualization–are the preferred tool for monitoring ice dynamics [8–13].

At present, studies of lake ice dynamics mainly focus on extracting and analyzing their spatiotemporal distribution and physical characteristics. For example, L.L. Sukhacheva [14] analyzed the spatiotemporal variations in ice conditions, ice formation and melting processes, and the evolution of ice morphology in the Gulf of Finland and the Neva Bay in 2011–2012. V.M. Kolyi [15] used satellite imagery to monitor river ice conditions from April 2013 to November 2017. Zh. Wang [16] studied lakes larger than 100 km² on the Tibetan Plateau and their changes during 2000–2015. M. Qi [17], using Terra MODIS and Landsat TM/ETM+, analyzed the ice characteristics of Qinghai Lake from 2000 to 2016, revealing a shortening of the ice-cover duration and identifying cumulative negative winter temperature as a key factor.

The latitudinal position and continental climate of Lake Kulinda determine the specific dynamics of its ice cover, but the study of this lake in this regard is clearly insufficient. This study uses Landsat-8 and Landsat-9 satellite images and GIS software to analyze the temporal changes in the ice cover of Lake Kulinda from 2019 to 2025, as well as the factors that influence the

a

b

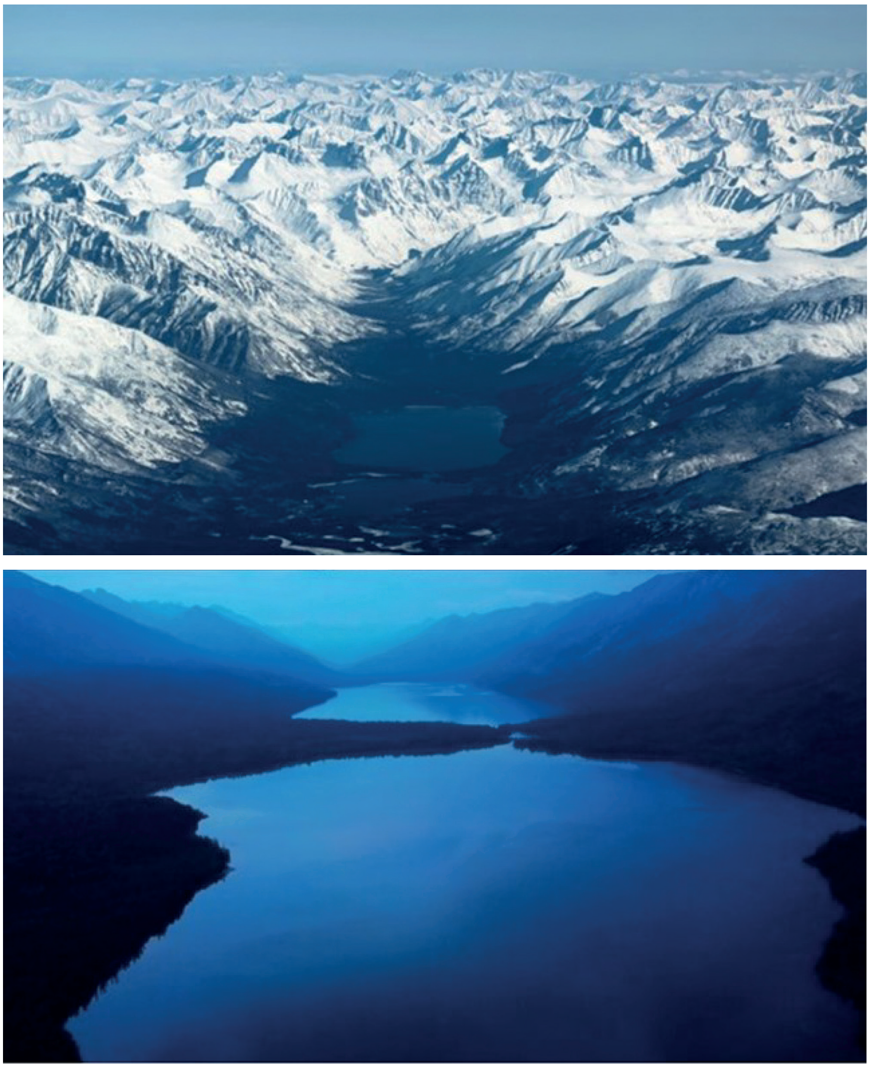

Fig. 2. Photos of Lake Kulinda in early autumn (a) and summer (b)
Рис. 2. Фотографии озера Кулинда ранней осенью (a) и летом (b)

evolution of ice cover in similar regions. The results obtained can be used in studies of the ice cover dynamics in Central Siberia as a whole.

Materials and methods

Lake Kulinda is located in the dryland part of the North Baikal Basin, with geographical coordinates of 56°06' N and 110°29' E (see Fig. 1). The lake belongs to the Kichera River basin and is a typical glacial lake, a relic of the last glaciation. The total surface area of the lake is 9.21 km² [18, 19]. The lake is elongated and has steep banks and a straight coastline.

The lake is surrounded by medium-high mountains (800–1,200 m) (see Fig. 2), with traces of large-scale glacial processing of the last glacial maximum: karst, troughs, glacial valleys, lateral, bottom, and terminal moraines. The bedrock is represented by Paleozoic and Mesozoic igneous and metamorphic formations, partially covered by glacial and lake deposits. The soils are mountain-tundra and cryogenic, with a thin humus layer and low fertility. The vegetation is typical for the territories of the Northern Baikal region and consists of tundra, shrubs, and rare coniferous forests.

The regional climate is cold temperate continental, strongly influenced by the Siberian High and polar air masses: long, very cold winters and short, cool summers. The mean annual temperature is well below 0°C. The average January temperature may fall below -30°C and sometimes to -45°C; the average July temperature is 10–15°C, and extremes do not exceed approximately 25°C. Annual precipitation is approximately 350–450 mm, mostly in the form of snow. Snow cover persists for more than 7 months (from mid-October to May). Wind conditions are usually strong, especially in winter, with frequent blizzards; wind action produces ridges and cracks on the ice [20].

These harsh conditions result in a long ice-cover period: freeze-up usually begins in early November and lasts until the end of May – about 6 months. Maximum ice thickness reaches 1–1.2 m, with local variations caused by snow cover and wind redistribution. May is a critical phase of melt phenology: rising temperature and increasing solar radiation initiate melting along the shore and over the ice surface. Therefore, analyzing interannual variability in ice area in May effectively reflects the influence of climate warming on the regional cryosphere [21].

Hydrologically, the lake is supplied mainly by atmospheric precipitation and snowmelt, and water levels are relatively stable. The water is clear; in summer, surface temperatures reach 10–12°C [22], while bottom waters remain stable at approximately 4°C, forming a two-layer thermal structure. Due to its remoteness, human impact is minimal, and the area retains a high natural status, making the lake a suitable site for studying ice dynamics at high latitudes.

Under global warming, Siberia is considered one of the most climate-sensitive regions, and changes in its cryosphere have attracted substantial scientific interest. As a representative glacial lake in the region, Lake Kulinda reflects local climate trends and serves as an important reference for understanding hydroclimatic changes in Baikal-type regions [23]. Therefore, an in-depth analysis of the spatiotemporal variations in the lake's ice cover has high scientific value and practical significance for understanding cryosphere-climate interactions at high latitudes and for predicting future changes.

Results and discussion

Normalized Difference Snow Index. The Normalized Difference Snow Index (NDSI) is a classical method for identifying snow and ice based on the spectral characteristics of reflectance in specific wavelength ranges.

NDSI exploits the high reflectance of snow/ice in the visible range and the low reflectance in the shortwave infrared (SWIR) to distinguish ice-covered and ice-free areas. It is calculated as:

$$NDSI = \frac{(band3 - band6)}{(band3 + band6)}.$$

NDSI is the normalized difference between the reflectance in the green band and the shortwave infrared band (SWIR1). For Landsat-8 and Landsat-9, the green band is band 3 (0.53–0.59 μm), and SWIR1 is band 6 (1.57–1.65 μm).

NDSI values range from -1 to +1: snow and ice are characterized by high values (close to +1), whereas open water produces negative or low values. Therefore, by selecting an appropriate threshold, ice can be effectively separated from water/ice-free areas. In this study, the Otsu's method was used as the thresholding method. Pixels with NDSI ≥ 0.42 were classified as ice, and the remaining pixels were classified as ice-free.

In this study, Landsat-8 and Landsat-9 imagery was used, in which band 3 is the green band and band 6 is the shortwave infrared band. The threshold for ice extraction was determined using a method similar to a single-band threshold approach. The optimal threshold calculated by the Otsu's method was set at 0.42. Areas with NDSI values greater than or equal to 0.42 were classified as ice, while areas with values below 0.42 were classified as ice-free.

Area calculation. Each pixel in remote sensing imagery represents a specific surface area of a given size. Therefore, the area of surface objects can be calculated by multiplying the number of pixels belonging to a given object by the area of a single pixel. This method is widely used in remote sensing because of its high accuracy in area estimation.

Using ArcGIS software, statistics were generated for pixel values in the classified remote sensing images in order to obtain all ice and ice-free pixels, on the basis of which the total areas of ice-covered and ice-free regions were calculated. The process is as follows:

1. Pixel statistics.

For the binary classification image generated in the previous step (where ice pixels are assigned a value of 1 and non-ice pixels a value of 0), statistical analysis of pixel values was performed. Using the raster attribute table function in ArcGIS, all pixels within the study area were extracted, and the total number of ice pixels N_{ice} and non-ice pixels $N_{non\text{-}ice}$ was calculated separately.

2. Area calculation.

Based on the spatial resolution of the remote sensing images, the actual areas of the ice-covered and ice-free regions were calculated using the formula:

$$A_{ice} = N_{ice} \times (GSD)^2;$$
$$A_{non-ice} = N_{non-ice} \times (GSD)^2,$$

where A_{ice} is the total ice area; $A_{non\text{-}ice}$ is the total ice-free area; *GSD* is the ground sampling distance (spatial resolution) of the images, expressed in meters per pixel.

The spatial resolution of the Landsat-8 and Landsat-9 multispectral bands is 30 m. Thus, the surface area represented by one pixel is 900 m². For clarity and ease of comparison, the calculated area is converted uniformly to square kilometers (km²) using the conversion factor: 1 km² = 10^6 m².

Accuracy and error assessment. All remote sensing classification methods are inherently associated with certain errors. The main sources of error in this study include mixed pixels and cloud influence.

Mixed-pixel problem: Along the ice-water boundary, a single 30×30 m pixel may contain both ice and water, producing an NDSI value between that of pure ice and pure water and potentially leading to misclassification.

Cloud and shadow influence: Although images without clouds were preferred, thin clouds and their shadows may alter the spectral response of the surface and affect NDSI values.

To assess and ensure the reliability of the results, the following measures were implemented:

1. Visual validation of interpretation. The NDSI classification results were overlaid on true-color composites for the same period. Classification boundaries were manually compared with visually distinguishable ice-water boundaries in the images. Clearly misclassified areas were recorded and analyzed to determine the reasons.

2. Temporal consistency check. Classification results for similar dates in different years were compared to verify the logical consistency of their spatial distributions (for example, ice retreat should generally occur from the shoreline toward the center of the lake). This helped eliminate anomalies caused by the quality of a single scene.

3. Verification of total area. The total area of ice and ice-free regions calculated in this study was compared with the known total area of Lake Kulinda (9.21 km²). This served as a reference for validating the overall correctness of the data-processing procedure.

Through a systematic and carefully applied methodology, information on the ice cover of

Lake Kulinda for 2019–2025 was extracted from Landsat-8 and Landsat-9 time-series imagery. A quantitative spatiotemporal analysis was conducted, establishing a data basis for the subsequent study of change patterns and driving mechanisms.

Results and analysis. Let's consider the spatiotemporal changes in the ice cover from 2019 to 2025 based on remote sensing data:

1. Spatiotemporal ice-cover data for 2019.

The image (Fig. 3) shows that on April 10, 2019, the ice cover on the lake was continuous and undamaged, covering the largest area compared to the images from 2019, 2021, 2023, and 2025. This dataset serves as an important baseline for subsequent change detection and quantitative analysis. At the same time, early signs of melting were observed along the southern margins.

2. Spatiotemporal ice-cover data for 2021.

Compared to the 2019 ice cover map (see Fig. 3), the data from April 8, 2021 (Fig. 4) show significant changes. The images reveal that the ice area has decreased, particularly along the edges of the ice mass. The largest reduction in ice area was observed in the eastern and western parts of the lake. In these areas, the boundary between ice and water has receded, becoming more irregular and discontinuous. These changes indicate a clear trend toward ice reduction in the study area during 2019–2021, reflecting ongoing melting and fragmentation of the ice cover.

3. Spatiotemporal ice-cover data for 2023.

The results of monitoring the April 14, 2023 image (Fig. 5) show that the trend of ice melting in the study area continues. Compared to 2019 and 2021, the most notable changes occurred in two aspects: first, the total area of the ice cover decreased, and the ice boundary shifted significantly inward in both the eastern and western parts of the lake; second, signs of melting appeared in the central part of the ice cover. This indicates that ice-cover degradation progressed from coastal shrinkage to internal melting.

4. Spatiotemporal ice-cover data for 2025.

The results of the analysis of the April 18, 2025 image (Fig. 6) show that the trend of degradation has continued compared to previous images. The once-dominant continuous ice mass was further reduced and fragmented into many smaller residual ice masses, indicating that the previous prevailing continuous ice-cover pattern was no longer present. At the same time, the image shows that over six years of spatiotemporal evolution, the surface-cover pattern of the study area underwent substantial change.

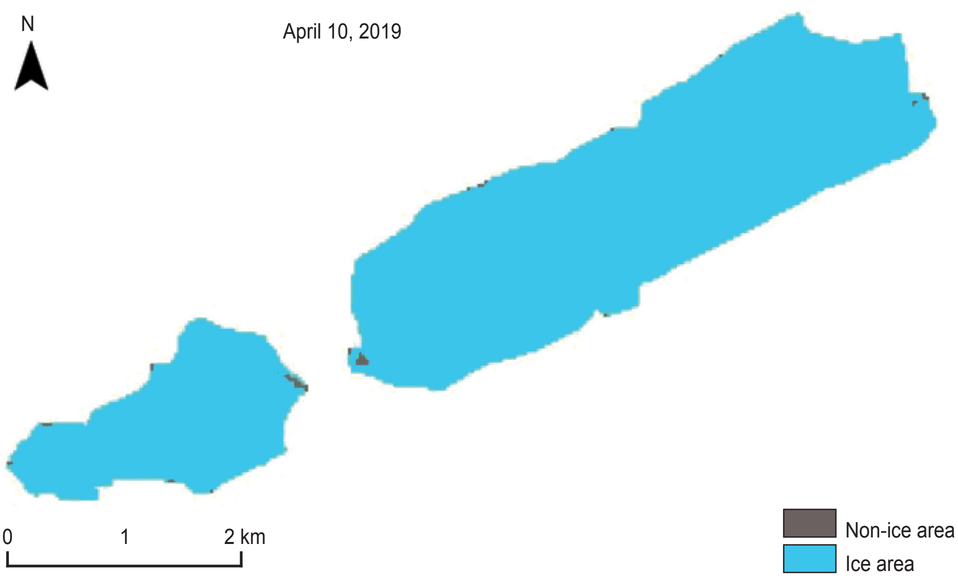

Fig. 3. Spatiotemporal characteristics of ice cover in 2019
Рис. 3. Пространственно-временные характеристики ледяного покрова в 2019 г.

Analysis of changes in 2019–2025. In this study, Landsat-8 and Landsat-9 images acquired on 2019, 2021, 2023, and 2025 were selected as the data source. Ice-cover information was extracted using the NDSI method, and binary maps of ice and ice-free areas were produced (see Figs 3–6).

The extraction results show a continuous decrease in the ice area of Lake Kulinda from 2019 to 2025, as detailed in Table. Specifically, the ice area was 9.17 km² in 2019, 9.09 km² in 2021, 8.93 km² in 2023, and 8.86 km² in 2025. Over the six-year period from 2019 to 2025, the total reduction in ice area was 0.31 km², corresponding to an average annual decrease of 0.05 km². Between 2019 and 2021, the ice area decreased by 0.08 km² (an average annual decline of 0.04 km²). From 2021 to 2023, the ice area decreased by 0.15 km² (an average annual decline of 0.08 km²), which was the largest drop among all observed intervals. Between 2023 and 2025, the ice area decreased by 0.07 km², with an average annual decline of 0.04 km².

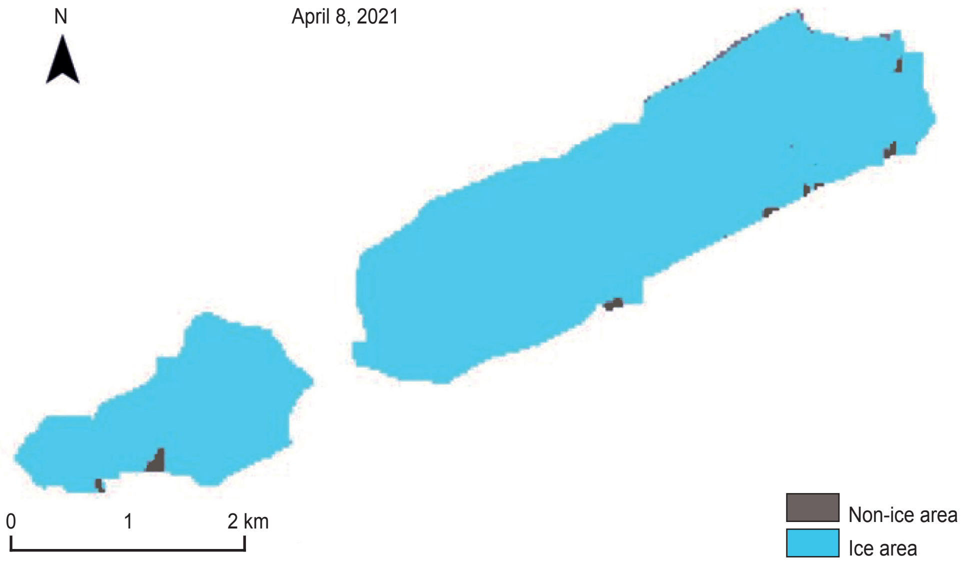

Fig. 4. Spatiotemporal characteristics of ice cover in 2021
Рис. 4. Пространственно-временные характеристики ледяного покрова в 2021 г.

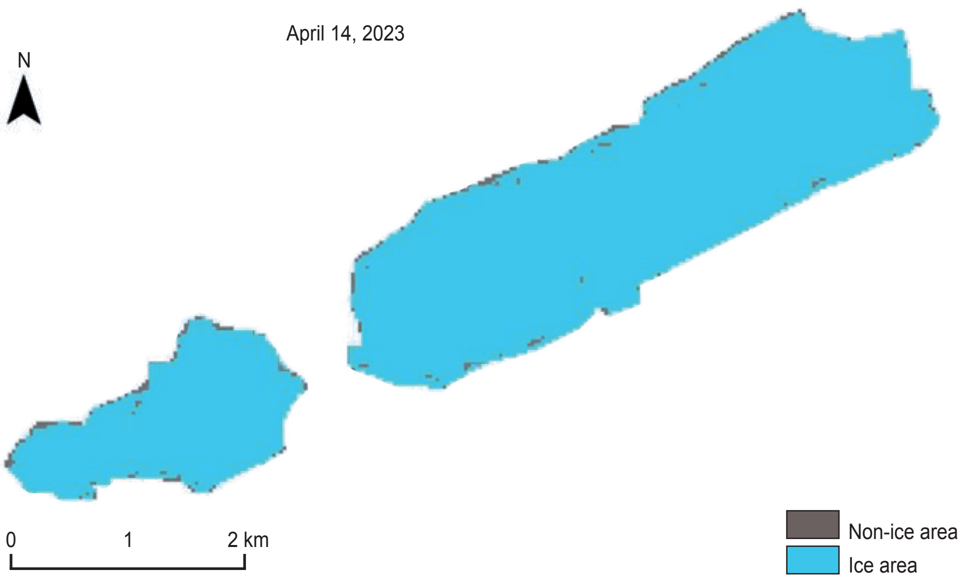

Fig. 5. Spatiotemporal characteristics of ice cover in 2023
Рис. 5. Пространственно-временные характеристики ледяного покрова в 2023 г.

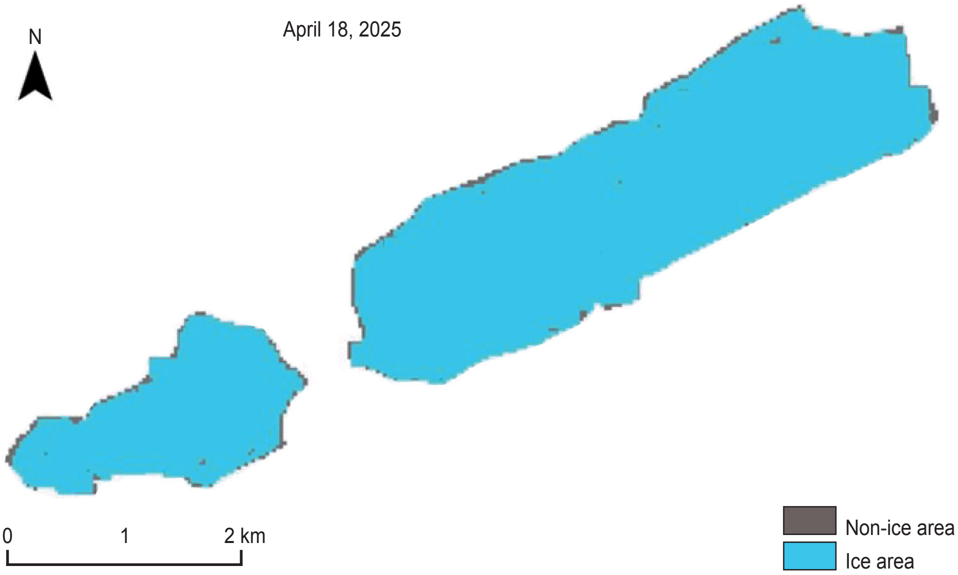

Fig. 6. Spatiotemporal characteristics of ice cover in 2025
Рис. 6. Пространственно-временные характеристики ледяного покрова в 2025 г.

Statistics of lake ice area of Lake Kulinda (2019–2025)
Статистические данные о площади ледового покрова озера Кулинда (2019–2025 гг.)

Year	Ice area, km²	Non-ice area, km²	Total area, km²	Changes in the ice area, km²	Average, km²
2019	9.1665	0.0441	9.2106	–	–
2021	9.087	0.1236	9.2106	-0.0795	-0.0398
2023	8.9341	0.2765	9.2106	-0.1529	-0.0765
2025	8.8596	0.351	9.2106	-0.0745	-0.0373

Conclusion

Based on Landsat-8 and Landsat-9 images acquired in April of each year from 2019 to 2025, this study monitored and analyzed the ice conditions of Lake Kulinda using the NDSI method. The main conclusions are as follows:

1. The ice area of Lake Kulinda showed a stable declining trend during the study period. The annual rate of ice loss first increased and then decreased; the smallest average annual decline was recorded in 2023–2025. This indicates that although the ice cover continues to shrink, the rate of reduction has slowed and is no longer characterized by abrupt change.

2. Ice melting occurred mainly along the shoreline, especially in the southeastern and northwestern coastal areas, while the central part of the ice cover remained relatively stable. Time-series analysis shows that the ice-water boundary retreated toward the center of the lake each year. In terms of area change, the greatest reduction occurred in 2021–2023, with an average annual decrease of 0.08 km²; by contrast, the average annual decrease slowed to 0.04 km² in 2023–2025, indicating a marked slowdown in ice retreat and a gradual stabilization of the melting process.

3. Comparison with meteorological data revealed a clear correlation between the decrease in ice area and the rise in regional temperature. The accelerated melting in 2021–2023 corresponded to a significant increase in spring temperatures in the area. The slowdown in ice loss after 2023 may be attributed to interannual climate variability and the nonlinear response of the ice system to climate change, reflecting a phase of adaptation and reorganization of the lake ice system under continued warming.

The authors believe that the research results can be used in monitoring the phenological state of the ice cover formation in the lakes of the Northern Baikal region, which will contribute to a better understanding of climate change in the region. These results can be significantly improved with a longer series of satellite observations and improved synchronization.

References

1. Frey H., Haeberli W., Linsbauer A., Huggel C., Paul F. A multi-level strategy for anticipating future glacier lake formation and associated hazard potentials. *Natural Hazards and Earth System Sciences*. 2010;10(2):339-352. https://doi.org/10.5194/nhess-10-339-2010.

2. Lützow N., Veh G., Korup O. A global database of historic glacier lake outburst floods. *Earth System Science Data*. 2023;15(7):2983-3000. https://doi.org/10.5194/essd-15-2983-2023.

3. Yan B., Jia H., Ren W., Wu R., Huang X. Glacier lake extraction and variation analysis of the Bujiagangri glacier based on the NDWI-NDSI combination threshold method. *National Remote Sensing Bulletin*. 2022;26(11):2344-2353. https://doi.org/10.11834/jrs.20210205.

4. Luo Z., Liu K., Zhang C., Deng X., Ma R., Song C. Progress of the DEM application for studying lake hydrologic dynamics. *Journal of Geo-Information Science*. 2020;22(7):1510-1521. https://doi.org/10.12082/dqxxkx.2020.190538.

5. Zhang C., Yao X., Li S., Liu L., Sha Te., Zhang Yu. Glacier change in the west Kunlun main peak area from 2000 to 2020. *Remote Sensing*. 2023;15(17):4236. https://doi.org/10.3390/rs15174236.

6. Mergili M., Pudasaini S.P., Emmer A., Fischer J.-T., Cochachin A., Frey H. Reconstruction of the 1941 GLOF process chain at Lake Palcacocha (Cordillera Blanca, Peru). *Hydrology and Earth System Sciences*. 2020;24(1):93-114. https://doi.org/10.5194/hess-24-93-2020.

7. Wang Q., Wang X., Lei D. The interaction mechanisms between mountain glacier evolution and glacial lake development. *Journal of Glaciology and Geocryology*. 2022;44(3):1041-1052. https://doi.org/10.7522/j.issn.1000-0240.2022.0097.

8. Zhang T., Wang W., Gao T., An B., Shang X. Glacial lake outburst floods on the High Mountain Asia: a review. *Journal of Glaciology and Geocryology*. 2021;43(6):1673-1692. (In Chinese). https://doi.org/10.7522/j.issn.1000-0240.2021.0066.

9. Main B., Copland L., Smeda B., Kochtitzky W., Samsonov S., Dudley J., et al. Terminus change of Kaskawulsh Glacier, Yukon, under a warming climate: retreat, thinning, slowdown and modified proglacial lake geometry. *Journal of Glaciology*. 2023;69(276):936-952. https://doi.org/10.1017/jog.2022.114.

10. Lavrova O.Yu., Mityagina M.I., Kostianoy A.G. Ice conditions in the Kerch strait in the current century. Retrospective analysis based on satellite data. *Current Problems in Remote Sensing of the Earth from Space*. 2017;14(2):148-166. (In Russ.). https://doi.org/10.21046/2070-7401-2017-14-2-148-166.

11. Higuchi Y., Setoyama D., Isegawa K., Tsuchikawa Y., Matsumoto Y., Parker J.D., et al. Pulsed neutron imaging for differentiation of ice and liquid water towards fuel cell vehicle applications. *Physical Chemistry Chemical Physics*. 2021;23(2):1062-1071. https://doi.org/10.1039/d0cp03887c.

12. Zhao F., Long D., Li X., Huang Q., Han P. Rapid glacier mass loss in the Southeastern Tibetan Plateau since the year 2000 from satellite observations. *Remote Sensing of Environment*. 2022;270:112853. https://doi.org/10.1016/j.rse.2021.112853.

13. Qayyum N., Ghuffar S., Ahmad H., Yousaf A., Shahid I. Glacial lakes mapping using multi satellite PlanetScope imagery and deep learning. *ISPRS International Journal of Geo-Information*. 2020;9(10):560. https://doi.org/10.3390/ijgi9100560.

14. Suhacheva L.L., Drabkin V.V., Ivanov V.V. Monitoring results of ice conditions in the Gulf of Finland, Neva Bay and in the area of the protective structures complex in the period 2011–2012. *Meteorologicheskii vestnik*. 2013;5(1):31-52. (In Russ.).

15. Koliy V.M., Agafonova S.A. The possibilities of using satellite data for the study of the ice cover of rivers. In: *The third Vinogradov readings. Facets of Hydrology: collected reports of the International scientific conference in memory of the outstanding Russian hydrologist Yuri Borisovich Vinogradov*. 28–30 March 2018, St. Petersburg. St. Petersburg: Naukoemkie tekhnologii; 2018, p. 48-52. (In Russ.).

16. Wang Z.Y., Wu Y., Chang J., Zhang X., Peng D. Temporal and spatial variation of lake ice phenology and its influencing factors in the Tibetan Plateau. *Journal of Beijing University of Technology*. 2017;43(5):701-709. https://doi.org/10.11936/bjutxb2016090032.

17. Qi M., Yao X., Li X., Duan H. Spatiotemporal characteristics of Qinghai Lake ice phenology between 2000 and 2016. *Journal of Geographical Sciences*. 2019;29(1):115-130. https://doi.org/10.1007/s11442-019-1590-5.

18. Wangchuk S, Bolch T. Mapping of glacial lakes using Sentinel-1 and Sentinel-2 data and a random forest classifier: strengths and challenges. *Science of Remote Sensing*. 2020;2:100008. https://doi.org/10.1016/j.srs.2020.100008.

19. Hu C., Lee Z., Franz B. Chlorophyll *a* algorithms for oligotrophic oceans: a novel approach based on three□band reflectance difference. *Journal of Geophysical Research: Oceans*. 2011;117(C1):C01011. https://doi.org/10.1029/2011JC007395.

20. Yang C., Wang X., Wei J., Zhang Y., Tang Z., Liu Q., et al. Chinese glacial lake inventory based on 3S technology method. *Acta Geographica Sinica*. 2019;74(3):544-556. https://doi.org/10.11821/dlxb201903011.

21. Boczoń A., Kowalska A., Stolarek A. The impact of climate change on the high water levels of a small river in Central Europe based on 50-year measurements. *Forests*. 2020;11(12):1269. https://doi.org/10.3390/f11121269.

22. Shrestha F., Steiner Ja.F., Shrestha R., Dhungel Ya., Joshi Sh.P., Inglis S., et al. A comprehensive and version-controlled database of glacial lake outburst floods in High Mountain Asia. *Earth System Science Data*. 2023;15(9):3941-3961. https://doi.org/10.5194/essd-15-3941-2023.

23. Luo S., Song C., Zhan P., Fan C., Liu K., Chen T., et al. Satellite laser altimetry reveals a net water mass gain in global lakes with spatial heterogeneity in the early 21st century. *Geophysical Research Letters*. 2022;49(3):e2021GL096676. https://doi.org/10.1029/2021GL096676.

Список источников

1. Frey H., Haeberli W., Linsbauer A., Huggel C., Paul F. A multi-level strategy for anticipating future glacier lake formation and associated hazard potentials // Natural Hazards and Earth System Sciences. 2010. Vol. 10. Iss. 2. P. 339–352. https://doi.org/10.5194/nhess-10-339-2010.

2. Lützow N., Veh G., Korup O. A global database of historic glacier lake outburst floods // Earth System Science Data. 2023. Vol. 15. Iss. 7. P. 2983–3000. https://doi.org/10.5194/essd-15-2983-2023.

3. Yan B., Jia H., Ren W., Wu R., Huang X. Glacier lake extraction and variation analysis of the Bujiagangri glacier based on the NDWI-NDSI combination threshold method // National Remote Sensing Bulletin. 2022. Vol. 26. Iss. 11. P. 2344–2353. https://doi.org/10.11834/jrs.20210205.

4. Luo Z., Liu K., Zhang C., Deng X., Ma R., Song C. Progress of the DEM application for studying lake hydrologic dynamics // Journal of Geo-Information Science. 2020. Vol. 22. Iss. 7. P. 1510–1521. https://doi.org/10.12082/dqxxkx.2020.190538.

5. Zhang C., Yao X., Li S., Liu L., Sha Te., Zhang Yu. Glacier change in the west Kunlun main peak area from 2000 to 2020 // Remote Sensing. 2023. Vol. 15. Iss. 17. P. 4236. https://doi.org/10.3390/rs15174236.

6. Mergili M., Pudasaini S.P., Emmer A., Fischer J.-T., Cochachin A., Frey H. Reconstruction of the 1941 GLOF process chain at Lake Palcacocha (Cordillera Blanca, Peru) // Hydrology and Earth System Sciences. 2020. Vol. 24. Iss. 1. P. 93–114. https://doi.org/10.5194/hess-24-93-2020.

7. Wang Q., Wang X., Lei D. The interaction mechanisms between mountain glacier evolution and glacial lake development // Journal of Glaciology and Geocryology. 2022. Vol. 44. Iss. 3. P. 1041–1052. https://doi.org/10.7522/j.issn.1000-0240.2022.0097.

8. Zhang T., Wang W., Gao T., An B., Shang X. Glacial lake outburst floods on the High Mountain Asia: a review // Journal of Glaciology and Geocryology. 2021. Vol. 43. Iss. 6. P. 1673–1692. https://doi.org/10.7522/j.issn.1000-0240.2021.0066.

9. Main B., Copland L., Smeda B., Kochtitzky W., Samsonov S., Dudley J., et al. Terminus change of Kaskawulsh Glacier, Yukon, under a warming climate: retreat, thinning, slowdown and modified proglacial lake geometry // Journal of Glaciology. 2023. Vol. 69. Iss. 276. P. 936–952. https://doi.org/10.1017/jog.2022.114.

10. Лаврова О.Ю., Митягина М.И., Костяной А.Г. Ледовая обстановка в Керченском проливе в текущем столетии. Ретроспективный анализ на основе спутниковых данных // Современные проблемы дистанционного зондирования Земли из космоса. 2017. Т. 14. № 2. С. 148–166. https://doi.org/10.21046/2070-7401-2017-14-2-148-166.

11. Higuchi Y., Setoyama D., Isegawa K., Tsuchikawa Y., Matsumoto Y., Parker J.D., et al. Pulsed neutron imaging for differentiation of ice and liquid water towards fuel cell vehicle applications // Physical Chemistry Chemical Physics. 2021. Vol. 23. Iss. 2. P. 1062–1071. https://doi.org/10.1039/d0cp03887c.

12. Zhao F., Long D., Li X., Huang Q., Han P. Rapid glacier mass loss in the Southeastern Tibetan Plateau since the year 2000 from satellite observations // Remote Sensing of Environment. 2022. Vol. 270. P. 112853. https://doi.org/10.1016/j.rse.2021.112853.

13. Qayyum N., Ghuffar S., Ahmad H., Yousaf A., Shahid I. Glacial lakes mapping using multi satellite PlanetScope imagery and deep learning // ISPRS International Journal of Geo-Information. 2020. Vol. 9. Iss. 10. P. 560. https://doi.org/10.3390/ijgi9100560.

14. Сухачева Л.Л., Драбкин В.В., Иванов В.В. Результаты мониторинга ледовых условий в Финском заливе, Невской губе и в районе комплекса защитных сооружений в период 2011–2012 гг. // Метеорологический вестник. 2013. Т. 5. № 1. С. 31–52.

15. Колий В.М., Агафонова С.А. Возможности использования космических снимков для исследования ледяного покрова рек // Третьи Виноградовские чтения. Грани гидрологии: сборник докладов международной научной конференции памяти выдающегося русского гидролога Юрия Борисовича Виноградова (г. Санкт-Петербург, 28–30 марта 2018 г.). СПб.: Наукоемкие технологии, 2018. С. 48–52.

16. Wang Z.Y., Wu Y., Chang J., Zhang X., Peng D. Temporal and spatial variation of lake ice phenology and its influencing factors in the Tibetan Plateau // Journal of Beijing University of Technology. 2017. Vol. 43. Iss. 5. P. 701–709. https://doi.org/10.11936/bjutxb2016090032.

17. Qi M., Yao X., Li X., Duan H. Spatiotemporal characteristics of Qinghai Lake ice phenology between 2000 and 2016 // Journal of Geographical Sciences. 2019. Vol. 29. Iss. 1. P. 115–130. https://doi.org/10.1007/s11442-019-1590-5.

18. Wangchuk S, Bolch T. Mapping of glacial lakes using Sentinel-1 and Sentinel-2 data and a random forest classifier: strengths and challenges // Science of Remote Sensing. 2020. Vol. 2. P. 100008. https://doi.org/10.1016/j.srs.2020.100008.

19. Hu C., Lee Z., Franz B. Chlorophyll *a* algorithms for oligotrophic oceans: a novel approach based on three-band reflectance difference // Journal of Geophysical Research: Oceans. 2011. Vol. 117. Iss. C1. P. C01011. https://doi.org/10.1029/2011JC007395.

20. Yang C., Wang X., Wei J., Zhang Y., Tang Z., Liu Q., et al. Chinese glacial lake inventory based on 3S technology method // Acta Geographica Sinica. 2019. Vol. 74. Iss. 3. P. 544–556. https://doi.org/10.11821/dlxb201903011.

21. Boczoń A., Kowalska A., Stolarek A. The impact of climate change on the high water levels of a small river in Central Europe based on 50-year measurements // Forests. 2020. Vol. 11. Iss. 12. P. 1269. https://doi.org/10.3390/f11121269.

22. Shrestha F., Steiner Ja.F., Shrestha R., Dhungel Ya., Joshi Sh.P., Inglis S., et al. A comprehensive and version-controlled database of glacial lake outburst floods in High Mountain Asia // Earth System Science Data. 2023. Vol. 15. Iss. 9. P. 3941–3961. https://doi.org/10.5194/essd-15-3941-2023.

23. Luo S., Song C., Zhan P., Fan C., Liu K., Chen T., et al. Satellite laser altimetry reveals a net water mass gain in global lakes with spatial heterogeneity in the early 21st century // Geophysical Research Letters. 2022. Vol. 49. Iss. 3. P. e2021GL096676. https://doi.org/10.1029/2021GL096676.

Information about the authors / Информация об авторах

Mengyao Gu,
Student, Master of Surveying and Mapping Engineering,
School of Surveying and Land Information Engineering,
Henan Polytechnic University,
Jiaozuo, China,
✉ gumengyao77@gmail.com
https://orcid.org/0009-0007-4171-8608
Гу Мэняо,
студент, магистр инженерной геодезии,
Школа геодезии и инженерии земельной информации,
Хэнаньский политехнический университет,
г. Цзяоцзо, Китай,
✉ gumengyao77@gmail.com
https://orcid.org/0009-0007-4171-8608

Xiangyu Meng,
Student, Master of Surveying and Mapping Engineering,
School of Surveying and Land Information Engineering,
Henan Polytechnic University,
Jiaozuo, China,
Mengxiangyu2001@outlook.com
https://orcid.org/0009-0006-8770-1679
Мэн Сянюй,
студент, магистр инженерной геодезии,
Школа геодезии и инженерии земельной информации,
Хэнаньский политехнический университет,
г. Цзяоцзо, Китай,
Mengxiangyu2001@outlook.com
https://orcid.org/0009-0006-8770-1679

Vladimir M. Zhulikov,
Student,
Baikal School of BRICS,
Irkutsk National Research Technical University,
Irkutsk, Russian Federation,
wowaahhh@mail.ru
https://orcid.org/0009-0000-3637-9567
Жуликов Владимир Михайлович,
студент,
Байкальский институт БРИКС,
Иркутский национальный исследовательский технический университет,
г. Иркутск, Российская Федерация,
wowaahhh@mail.ru
https://orcid.org/0009-0000-3637-9567

Vitaliy L. Ruposov,
Cand. Sci. (Geol. & Mineral.), Associate Professor,
Associate Professor of the Department of Mine Surveying and Geodesy,
Institute of Subsoil Use,
Irkutsk National Research Technical University,
Irkutsk, Russian Federation,
ruposov@istu.edu
https://orcid.org/0000-0003-2202-9034
Рупосов Виталий Леонидович,
кандидат геолого-минералогических наук, доцент,
доцент кафедры маркшейдерского дела и геодезии,
Институт недропользования,
Иркутский национальный исследовательский технический университет,
г. Иркутск, Российская Федерация,
ruposov@istu.edu
https://orcid.org/0000-0003-2202-9034

Contribution of the authors / Вклад авторов

Mengyao Gu – investigation, methodology, formal analysis, validation, visualization, writing – original draft.
Xiangyu Meng – investigation, methodology, formal analysis, validation, visualization, writing – original draft.
Vladimir M. Zhulikov – data curation, writing – editing.
Vitaliy L. Ruposov – conceptualization, project administration, resources.
М. Гу – проведение исследования, разработка методологии, формальный анализ, валидация результатов, визуализация, написание черновика рукописи.
С. Мэн – проведение исследования, разработка методологии, формальный анализ, валидация результатов, визуализация, написание черновика рукописи.
В.М. Жуликов – курирование данных, редактирование рукописи.
В.Л. Рупосов – разработка концепции, административное руководство исследовательским проектом, предоставление ресурсов.

Conflict of interests / Конфликт интересов

The authors declare no conflict of interests.
Авторы заявляют об отсутствии конфликта интересов.

The final manuscript has been read and approved by all the co-authors.
Все авторы прочитали и одобрили окончательный вариант рукописи.

Information about the article / Информация о статье

The article was submitted 22.04.2026; approved after reviewing 07.05.2026; accepted for publication 18.05.2026.
Статья поступила в редакцию 22.04.2026; одобрена после рецензирования 07.05.2026; принята к публикации 18.05.2026.